PHYSICAL MODEL TEST AND CFD-SIMULATION OF AN ASYMMETRICAL THROTTLE IN A T-SHAPED JUNCTION OF A HIGH-HEAD POWER PLANT

Boris Huber
Institute of Hydraulic Engineering, Vienna University of Technology,
Karlsplatz 13/222, 1040 Vienna, Austria
phone: +43 1 58801 22211, e-mail: boris.huber@kw.tuwien.ac.at

ABSTRACT

Hydraulic model tests were conducted to evaluate the head-losses and flow conditions of an asymmetrical throttle in a surge chamber system of an Austrian high-head power plant. The asymmetrical throttle is situated at the beginning of the rising shaft of the surge tank in one of the three branches of a T-shaped junction. Due to the asymmetrical shape of the throttle it causes different head-losses between up- and downsurging water levels.

Several hydraulic model tests with a scale of 1:21 were carried out under different flow conditions to evaluate the head-losses. Due to the complex shape of the T-junction the model was milled out of a plastic cube with the help of CNC.

Then, several CFD-simulations were conducted in order to evaluate under which circumstances the CFD-simulation is able to give reasonable results.

Keywords: Physical model test; T-Junction; Hydraulic experiments; Throttle; CFD-simulation;

33rd IAHR Congress: Water Engineering for a Sustainable Environment

ISBN: 978-94-90365-01-1

1 INTRODUCTION

The hydraulic properties of an asymmetrical throttle are investigated in this paper. The throttle is situated in one branch of a T-shaped junction in the surge tank system of a projected high-head power plant. Physical model test were conducted to evaluate the head-losses and CFD-simulations were carried out and compared with the experiments in order to find out under which circumstances the CFD-simulation can give reasonable results.

The main branch of the T-junction is bended: one branch leads down to the pressure shaft inclined by 42° and has a circular shape with a diameter of 3.60 m (branch 'a'), the second branch has a horse-shoe like shape, is horizontal and has a diameter of 7.20 m (branch 'c'). Between these cross-sections the junction is bended and expands from 3.60 m up to 7.20 m. Adjacent to the horizontal branch the cross-section changes from a circular to a horseshoe-like shape. Some metres from there the branching leg of the T-junction diverts perpendicular to the bends' axis (branch 'b'). Here, the asymmetrical throttle is situated (see Fig. 1).

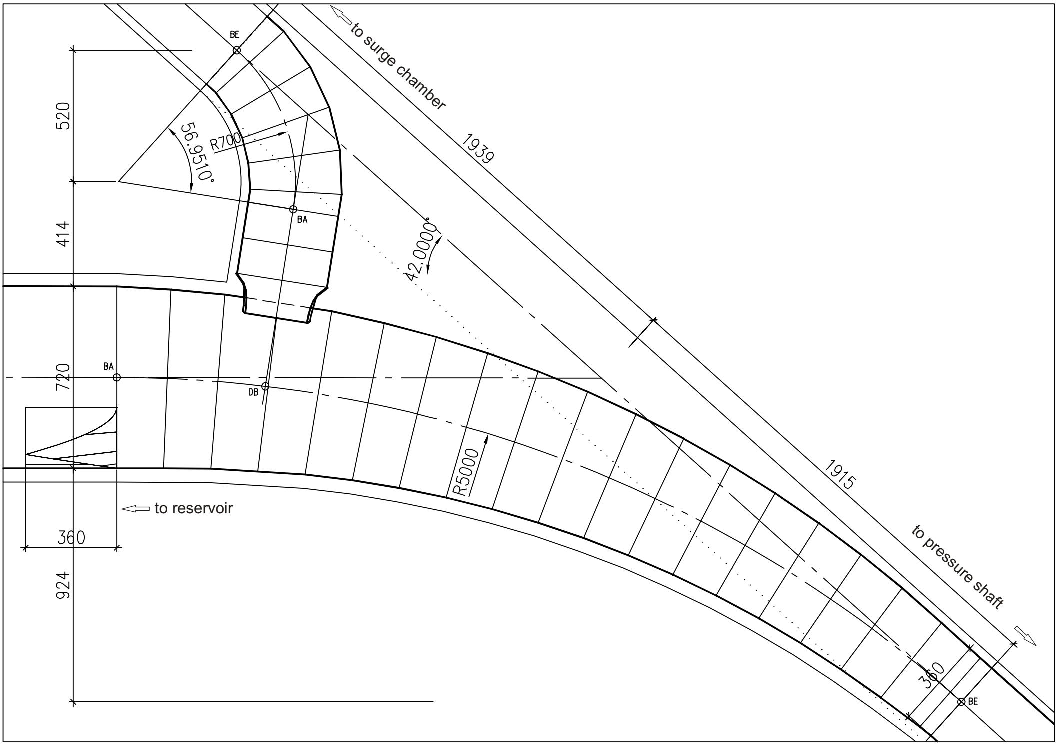

Fig. 1 – Vertical section of the bended T-junction (dimensions of prototype; in cm)

Fig. 2 shows a 3d-illustration of the throttle and the bended T-junction.

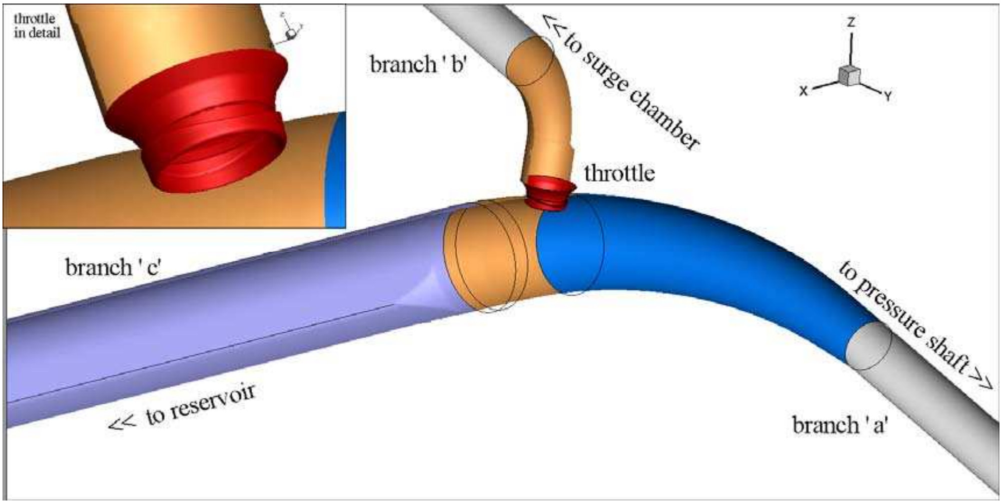

Fig. 2 – 3d-illustration of the throttle

1.1 Operating conditions

Seven different operating conditions had been examined (see Fig. 2 and Table 1)

case	description	branch 'a'	branch 'b'	branch 'c'
1	100% inflow from reservoir 100% to surge chamber	0	--	++
2	100% inflow from reservoir 50% to surge chamber, 50% to pressure shaft	-	-	++
3	100% inflow from pressure shaft 100% to surge chamber	++	--	0
4	100% inflow from pressure shaft 50% to surge chamber, 50% to reservoir	++	-	-
5	100% inflow from surge chamber 100% to reservoir.	0	++	--
6	100% inflow from surge chamber 100% to pressure shaft.	--	++	0
7	100% inflow from surge chamber 50% to reservoir, 50% to pressure shaft	-	++	-

Table 1 – definition of operating conditions
(++ inflow 100%, -- outflow 100%, - outflow 50%, 0 no flow)

2 Physical model tests

The scale of 1:21 was selected for the model tests. Due to the complex shape of the bended T-junction the model was milled out of 2 blocks of rigid foam plastic with the help of CNC. Between the two semi-shells, which were firmly fastened together, the throttle made of aluminum was placed to its position in the branching leg. The whole system was laid out horizontally (thus turned around 90°). This is a common method with this kind of model, as the influence of gravity is insignificant and the model is easier to handle.

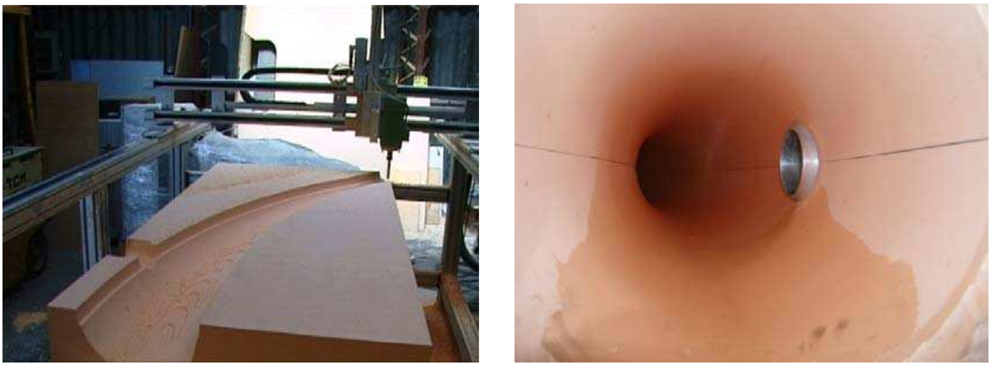

Fig. 3 – milling of the junction (left); throttle (right)

The pipes adjacent to the T-junction were made of plexiglass and had a diameter of 172 mm and 348 mm respectively. To achieve a uniform inflow, honeycombs had been situated in the inlet pipes and the lengths of the pipes were greater than 10xD: the smaller pipes were 2 m long and the horseshoe-shaped branch 4 m long (see Fig. 4). Discharge and pressure conditions according to the particular load-case were adjusted with slide valves.

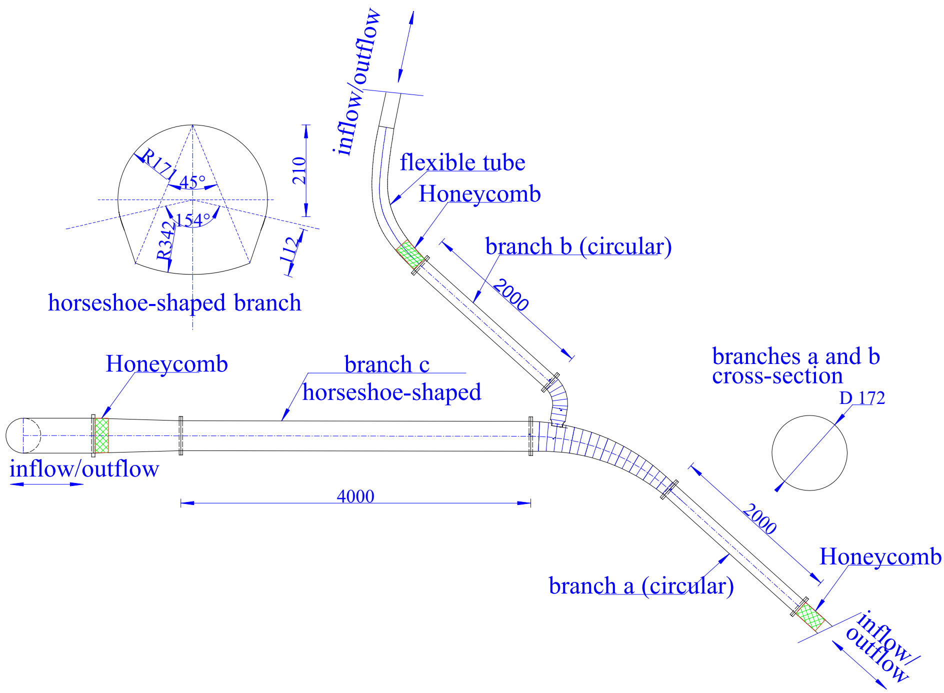

Fig. 4 – sketch of the experimental set-up (dimensions in mm)

Flow was measured with magnetic-inductive flow meters. Fig. 5 shows a photo of the experimental setup.

Fig. 5 – Photo of the experimental set-up

To measure pressure, 2 measuring-sections were situated at every branch, one near the T-junction and the other one at the end of the pipe, so that the distance between the junction and the downstream pressure gauge was more than 10xD and thus the pressure-field was almost constant.

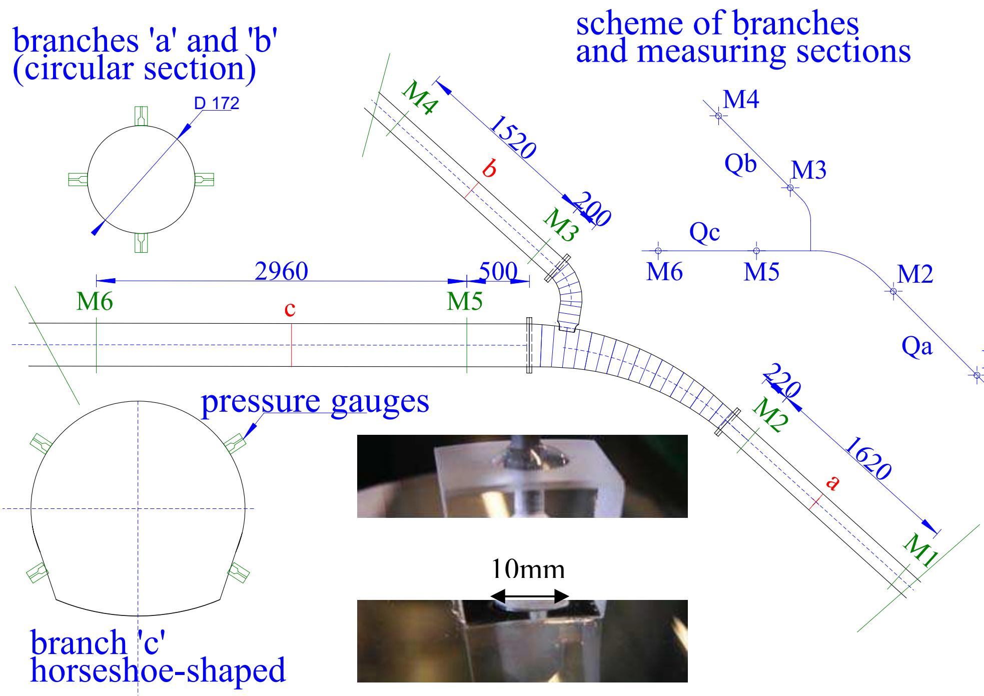

Fig. 6 – arrangement of pressure measuring sections

4 small bore holes (diameter 1.5 mm), which were connected by flexible hose-pipes, were placed in every measuring section, so that the measured pressure had an average value of the cross section. The hosepipes were connected to a difference-pressure meter and the pressure differences were recorded with a sample rate of 50 Hz.

2.1 Experimental results

The head-loss coefficient is determined by:

$$K_{ij} = \frac{total\ pressure\ \ in\, leg\ i - total\ pressure\ \ in\, leg\ \ j - pipe\ friction\ \ from\, i\ to\ j}{v_{Dr}^2 / 2g}$$

with v_{Dr} … mean velocity in smallest throttle-cross section (i.e. D_{Dr} = 2.47 m in Nature / 0.117 m in Model). Friction loss was calculated with a wall roughness of k=0.0015 mm and a kinematic viscosity of $\nu = 1.1e\text{-}6$ m²/s. Total pressure was gained by adding the velocity head ($v^2/2g$) to the measured pressure difference (Miller, 1978).

Depending on the specific load case, discharge was between 20 l/s and 90 l/s in the Model – corresponding Reynolds numbers were between $5 \cdot 10^5$ and $2 \cdot 10^6$ related to v_{Dr}. In all cases the loss coefficient either was almost constant or approached to a constant value with increasing discharge. The loss-coefficients were extrapolated to the prototype values (see Klasinc et al. 1992) and are summarized in Table 2.

case	Q_{Dr} / Q_{total}	$K_{2\text{-}6}$ resp. $K_{5\text{-}1}$ (not going through throttle)	$K_{2\text{-}4}$ resp. $K_{3\text{-}1}$ (going through throttle)
case 1	1.0	$\zeta_{5\text{-}1} = 0.03$	$\zeta_{5\text{-}4} = 1.60$
case 2	0.5	$\zeta_{5\text{-}1} = 0.05$	$\zeta_{5\text{-}4} = 1.63$
case 3	1.0	$\zeta_{2\text{-}6} = 0.07$	$\zeta_{2\text{-}4} = 1.72$
case 4[1]	0.5	$\zeta_{2\text{-}6} = 0.23$	$\zeta_{2\text{-}4} = 2.20$
case 5	1.0		$\zeta_{3\text{-}6} = 1.00$, $\zeta_{3\text{-}1} = 0.97$
case 6	1.0		$\zeta_{3\text{-}6} = 0.95$, $\zeta_{3\text{-}1} = 1.04$
case 7	0.5		$\zeta_{3\text{-}6} = 1.04$, $\zeta_{3\text{-}1} = 1.06$

Table 2 – summary of extrapolated loss-coefficients from experiments

The loss-coefficients gained from the experiments are depicted later in Fig. 8 to Fig. 11, together with the results of the CFD-simulations.

[1] Loss-coefficients are based on the velocity in the throttle – with the same throttle discharge, the flow through branch ‘a’ (and the velocity) in case 4 is twice as much as in case 3. Thus, velocity-head and total pressure in branch ‘a’ in case 4 are much higher than in case 3, and therefore the loss-coefficient is higher.

3 CFD-Simulation

3.1 Mesh and simulation parameters

The CFD-simulations were carried out with fluent 6.3.26. Most of the simulations were done in the scale of the physical model (1:21.05). The Realizable k-ε model was mainly used with standard pressure-discretization and first-order upwind scheme for momentum, k and ε equations (see fluent 6.3.26 manual for details).

In general, the near-wall zone was modelled with the standard wall function. The size of the near-wall cells with about 2 mm was chosen so that the height was sufficiently small to fulfill the required constraints (y+ between 50 and ca. 800).

Several simulations with different meshes were carried out in order to check the mesh independence. Fig. 7 shows details of one of the used meshes as an example.

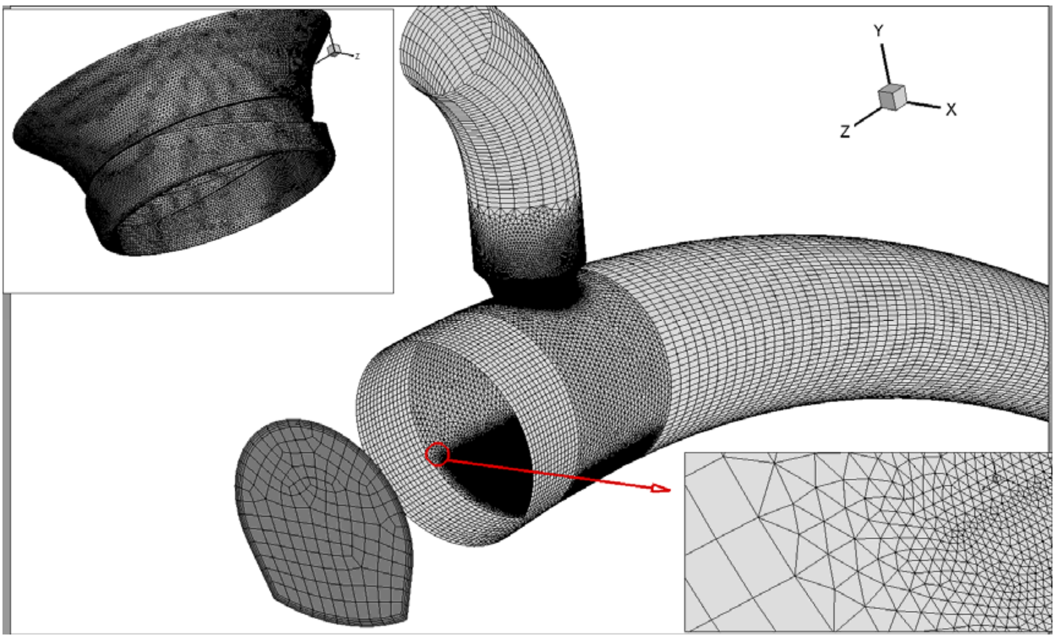

Fig. 7 – mesh details

3.2 Results of the CFD-simulations

For all cases mentioned above, several CFD-simulations had been carried out with different fluxes. In cases 1-4 the loss-coefficients in the CFD-simulations agreed well with the experimental results (see
Fig. 8 to Fig. 9).

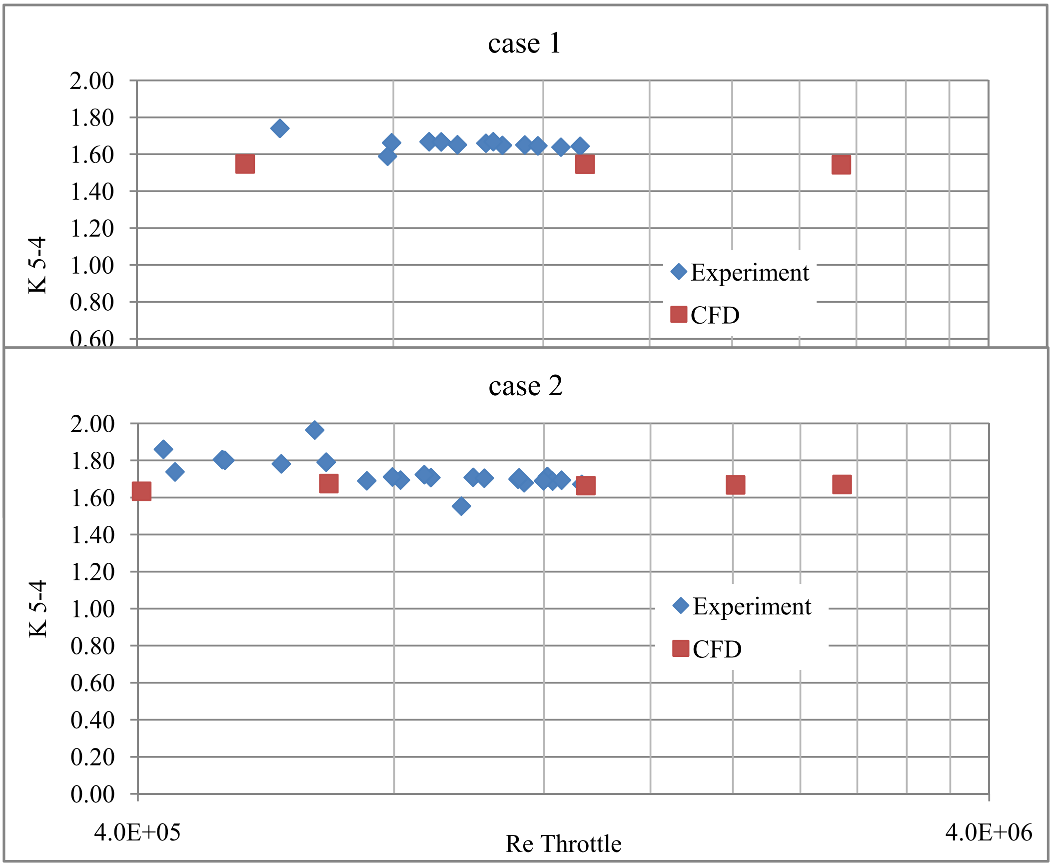

Fig. 8 – loss-coefficients K 5-4 case 1 and 2

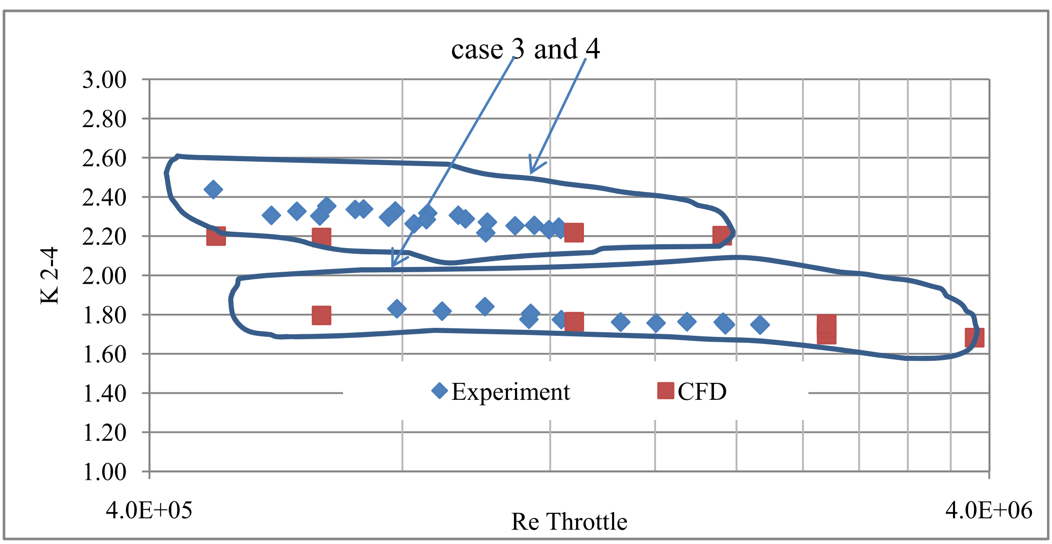

Fig. 9 – loss-coefficients case 3 and 4

In case 5 to 7 the results of the CFD simulations differed from the experiments: in the CFD simulations the loss coefficients were about 20% higher than in the experiments. As an example, the results for case 7 are depicted in Fig. 10 and Fig. 11.

In case 5-7, when flow is directly impinging on the wall opposite the throttle, it may be necessary to resolve the boundary layer in order to achieve exact results – but this can hardly be done in this case, dealing with a very complex geometry, pipe dimensions of some metres and high Reynolds numbers. However, some simulations had been carried out with y^+-values between 2 and 10 and usage of turbulence models able to resolve the boundary layer (k-ω-model) - but the loss coefficients did not change. It seems that the CFD-simulation comes upon the limits in this case.

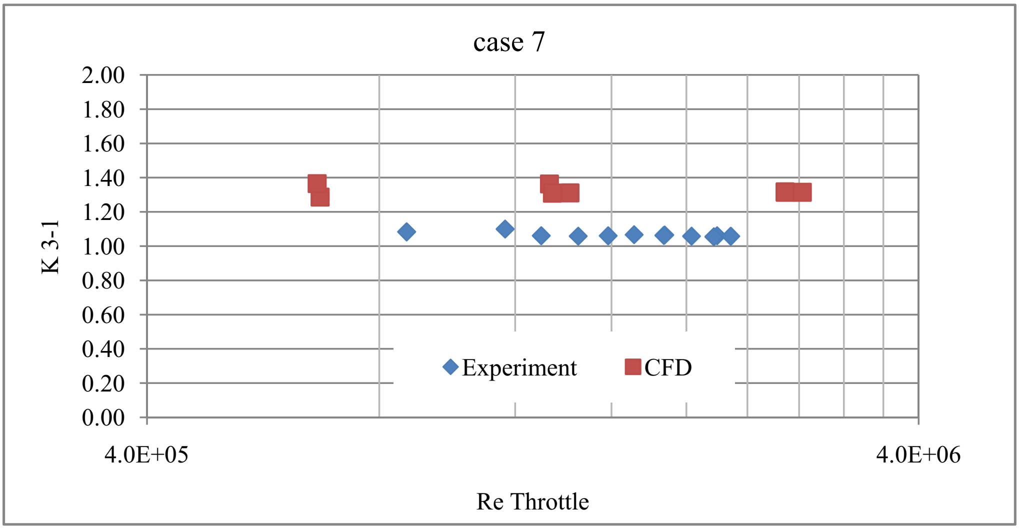

Fig. 10 – loss-coefficients K3-1 case 7

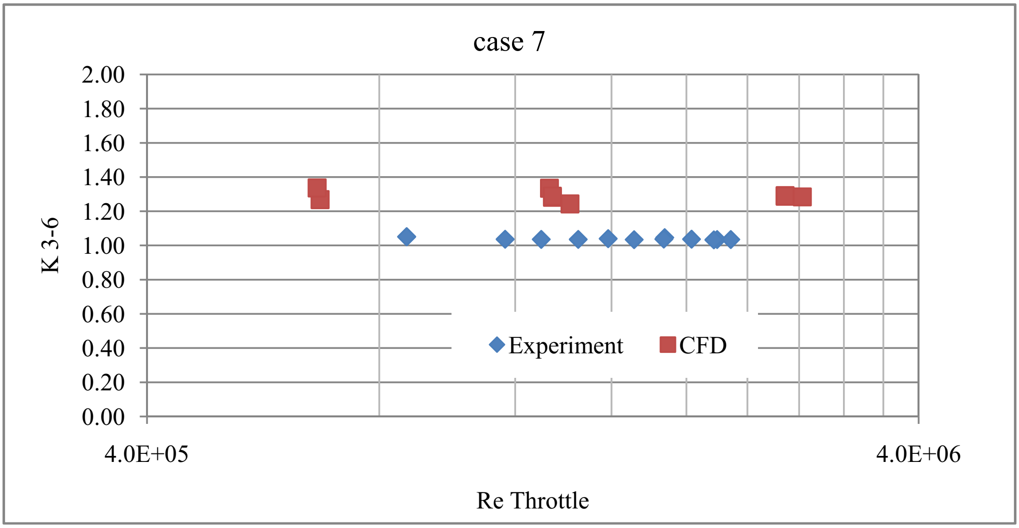

Fig. 11 – loss-coefficients K3-6 case 7

4 References

Kobus H., „Wasserbauliches Versuchswesen“, Dt. Verband für Wasserwirtschaft, Mitteilungsheft 4 (1978), 1978

Miller D:S:, “Internal Flow Systems”, BHRA Fluid Engineering, Vol.5, 1978

Klasinc R., Knoblauch H., Dum T., „Power Losses in Distribution Pipes“, 4th International Conference Hydrosoft 92, Valencia, 1992

Fluent 6.3 manual